Numerical Analysis and Preliminary Experimental Validation of a Heteropolar Electrodynamic Bearing

V. Kluyskens [1], B. Dehez [1], C. Dumont, A. Musolino [2], and R. Rizzo [2]

[1] Université Catholique de Louvain, Center for Research in Mechatronics, Louvain, Belgium
{virginie.kluyskens; bruno.dehez}@uclouvain.be

[2] University of Pisa, DESTEC, Department of Energy and Systems Engineering, Italy
{antonino.musolino; rocco.rizzo}@unipi.it

Abstract ─ In this paper we describe the numerical simulations of a Heteropolar Electrodynamic Bearing and compare them with some experimental data taken on a prototype in quasi-static state. The device is composed of a cylindrical permanent magnet rotor and six coils fixed onto the stator. The system has been simulated by means of a dedicated numerical code ("EN4EM" - Electric Network for Electromagnetics), previously developed for research purposes. The software is based on a 3D integral formulation and it is able to numerically simulate coupled multi-degree of freedom electro/mechanical problems. The comparison between computed and measured data are fully satisfactory.

Index Terms ─ Coupled analysis, electrodynamic bearings, integral formulation, permanent magnets.

I. INTRODUCTION

The modern technologies of Magnetic Levitation systems (MAGLEV) allow developing contact-free bearings which are appealing in many technological applications like high-speed drives, high-precision or vacuum devices, and so on [1]. Active magnetic bearings [2] offer great possibilities in terms of control and can achieve high stiffness. Although they operate quite well, some drawbacks, such as the complexity, overall dimensions, and cost of the control system, limit their diffusion. On the other hand, passive magnetic bearings [3], which do not require control system, seem to be a valid alternative. Unfortunately, passive magnetic suspensions suffer from the intrinsic instability (Earnshaw's theorem [4]) and great efforts must be devoted to design reliable stabilization devices.

Passive Electrodynamic Bearings (EDBs) belong to the latter category [5]. The EDBs can be classified into two groups depending on whether the magnetic field produced by the permanent magnets (PM) is homopolar or heteropolar. In these devices the forces that restore the rotor in the equilibrium position arise from currents induced by the relative motion between the permanent magnets and the conductive parts of the bearing. In many cases the null-flux coils can be used in order to achieve a higher energy efficiency [6]. In such kind of configurations, when the rotor is in the equilibrium position, the coils experience no varying magnetic flux and no current flows in the system. On the contrary, if the rotor is not in the equilibrium position the varying magnetic flux produces a non-zero electromotive force and consequently a current flows in the coils. Then, if properly designed, a restoring force can be obtained, allowing the rotor to come back to its equilibrium position. To properly design null flux centering heteropolar EDB, guidelines are given in [6]: the identity $q = p \pm 1$ has to be respected, where q and p are the number of pole pairs of the winding and permanent magnets, respectively.

In order to design passive magnetic bearings and to investigate their performance, many analytical and numerical models have been developed [7]–[12].

However, they have some limitations especially when dealing with the dynamic operation of electro-mechanical systems, under six degree of freedom (DOF). Also the application of the finite-element method (FEM) to systems with moving conductors presents some difficulties, mainly due to the coupling of meshes attached to bodies in relative motion [13]. They usually require a large number of unknowns to obtain a desired accuracy in multi-degree of freedom problems [14]. Moreover, the meshes and consequently the matrices involved in the calculations have to be updated during the motion and the analysis of unbounded domains requires special treatments [15].

In this paper an alternative approach is used to develop a numerical model capable to investigate the complex operation of passive magnetic bearings. This approach is based on an integral formulation [16] in which the problem of coupling moving meshes does not arise since only the discretization of the active regions is required. However, the integral formulations also present some limitations, usually related to the numerical

Submitted On: July 20, 2018
Accepted On: December 14, 2018

solution of the model. In fact, the main drawbacks are the matrix setup time and matrix solution time. The paper is organized as follows: the proposed device, and the numerical formulation are described in Sections II and III. Section IV briefly describes the test bench, while Section V discusses the comparison between the computed and the experimental data.

II. PROPOSED DEVICE

The Heteropolar Electrodynamic Bearing under investigation with the main dimensions is shown in Figs. 1 and 2.

The main characteristics of the device are:

- The rotor is a 1 pole pair annular NdFeB magnet, with diametrical magnetization and remanence Br=1.3 T.
- The stator is composed of a 3-phase system with 2 pole pairs. Each phase is made of series connection of 2 coils, in the way that when the rotor is perfectly centered the induced electromotive force (EMF) is zero, respecting criteria given in [6]. Each coil has 560 turns of 0.2 mm copper wire. There is no ferromagnetic yoke behind the coils.
- The nominal airgap when the rotor is centered is 4 mm.

The analysis of the system requires the use of numerical models able to simulate coupled electro/mechanical problems with up to six degree of freedom (6 DOF).

III. THE NUMERICAL FORMULATION

The device has been analyzed by means a numerical code ("EN4EM" - Electric Network for Electromagnetics), previously developed for research purposes [17]. It is based on a 3D integral formulation that reduces the diffusion equation to an equivalent network with time varying parameters. The values of the parameters in the electrical equations are function of the position of the rotor. The equations describing the rotor dynamics with 6 DOF are inherently nonlinear because of the dependence of the force on the position of the rotor itself.

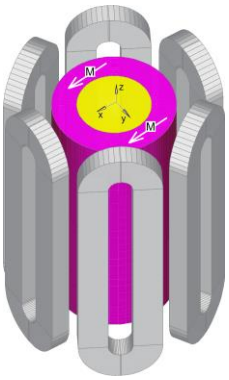

Fig. 1. A 3D view of the analyzed device.

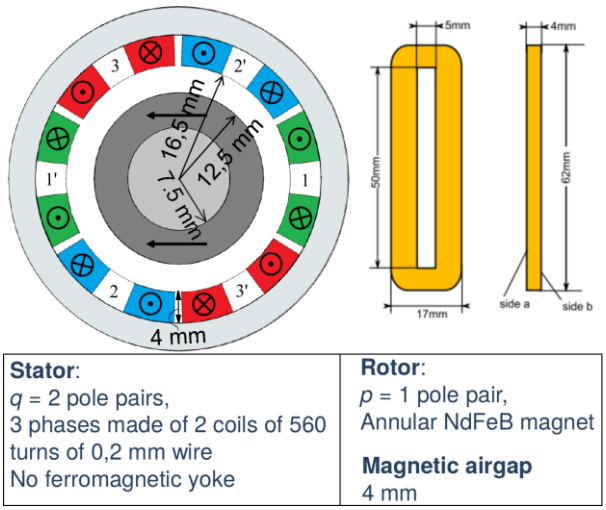

Fig. 2. Cross section and coils dimensions.

Furthermore, the problem of rigid body dynamics is coupled with the diffusion equation of the magnetic field. The main numerical formulation characteristics are: (a) only active (usually conductive) parts of a device must be discretized; (b) coupling with external lumped circuits is straightforward. The main drawbacks, instead, are the matrix setup time and the matrix solution time. These matrices are densely populated, and this may require (relatively) long computational times to get the solution. Anyhow, since this formulation is highly parallelizable, recent improvements in multicore CPUs or GPUs, allows to reduce the computation time.

The details of the adopted formulation and the development of a C-code exploiting the GPGPU Nvidia CUDA libraries is extensively described in [17].

Figure 3 shows the mesh used by the EN4EM numerical code to simulate the Heteropolar Electro-dynamic Bearing. The whole system has been discretized with 500 elementary volumes and the time to simulate the system at a fixed out-centered position and at a given angular speed was about 120 s.

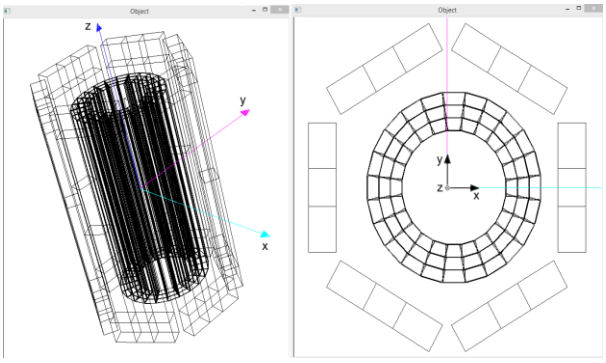

Fig. 3. The mesh used by the numerical code EN4EM to simulate the device.

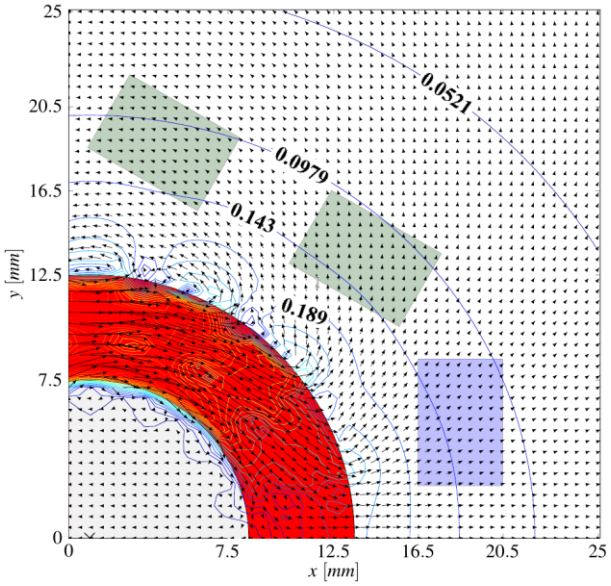

Fig. 4. The magnetic flux density B vectors in the system (dx=1 mm), produced only by the PM.

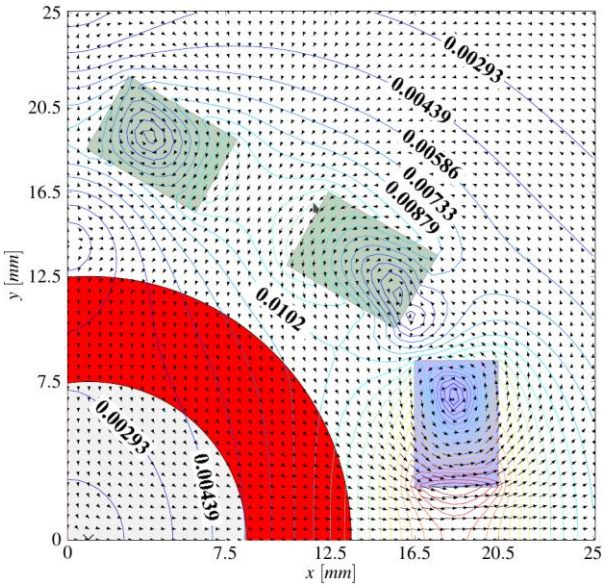

Fig. 5. The magnetic flux density B vectors in the system (dx=1 mm), produced only by the currents induced in the coils when the rotor spins at 7200 rpm. The currents in the coils are: $i_1=0.096$ *A*, $i_2=i_3=-0.047$ *A*. Coils are numbered according to Fig. 2.

As an example of software capabilities, Fig. 4 and 5 show the magnetic flux density vectors in the symmetry plane (z=0) of the system obtained by using the EN4EM code (for the sake of readability only a quarter of the system is shown). Although the code is able to simulate all the 6 DOF, in order to allow the comparison with the experimental results, the rotor has been constrained in some fixed out-centered positions. Then, several configurations of the device have been simulated by varying the spin speed and the center shift along the x and y directions. Other applications of the codes are reported in [17-20].

IV. THE TEST BENCH

The test bench is designed to operate in quasi-static conditions, i.e., the rotor spins in a fixed out-centered position relatively to the stator. Although the test bench was initially designed to operate up to 60.000 rpm, in order to reduce vibrations it has been used up to 7200 rpm only [21]. The rotor is driven by an external motor. The stator coils are glued inside a plastic structure. This plastic structure is mounted on a xy manual stage, allowing displacing the stator with respect to the rotor with a micrometer precision. The prototype is encased inside an enclosure for safety. The test bench is also equipped with a 6-axis force sensor, measuring the reaction forces on the stator winding. The test bench, with the safety enclosure opened, is represented in Fig. 6.

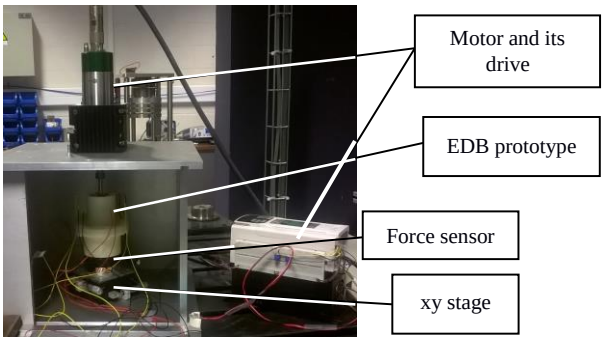

Fig. 6. The test bench.

V. RESULTS

The numerical formulation described in Section 3 has been used to perform the analysis of the described device operating under different conditions.

A first set of simulations has been performed in order to investigate the induced EMF in the open-circuited coils, as a function of spin speed and for different center shifts. Figure 7 shows the comparison between the computed results and the experimental data of the resultant induced EMF at the series connection of coils 1 and 1' (connected with discordant fluxes) as a function of time for a center shift *dx=1* mm and at a spin speed of 6000 rpm (counterclockwise). The results are fully satisfactory. Figure 8 reports the induced EMF (peak-to-peak) as a function of the center shift dx at the speed of 7200 rpm. The results show that the maximum errors obtained in the comparison with the experimental measurements are below 4%, confirming a good agreement between the simulations and the experimental

data. The computed results for $V_2(dx)$ and $V_3(dx)$ differ from those of $V_1(dx)$ for less than 1% and are not reported in the figure.

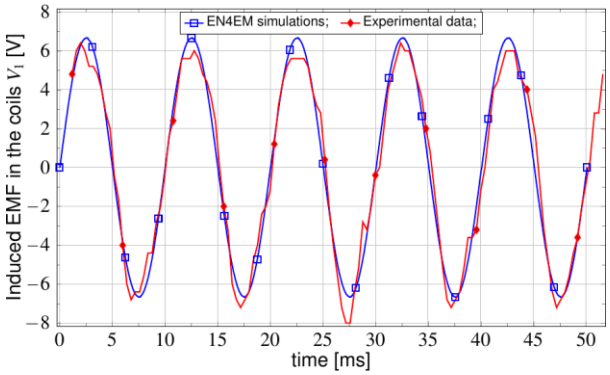

Fig. 7. Induced EMF V_1 in the (open-circuited) coils 1 1' as a function of time (dx=1mm, @6000 rpm).

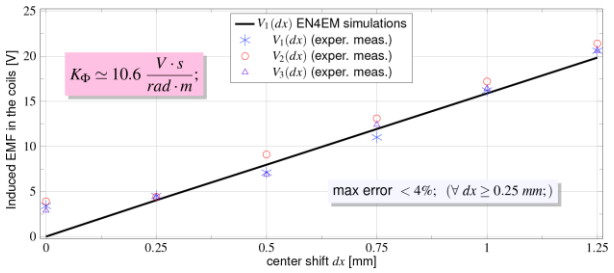

Fig. 8. Induced EMF in the (open-circuited) coils as a function of center shift dx (@7200 rpm).

The induced EMF should be zero when the rotor is centered, referring to the null-flux criterion, and it can be observed in Fig. 8 that it is indeed the case for the numerical model but not for the experimental data. This is due to some asymmetry between the phases, due for instance to their geometric precision, which leads to a magnetic center which is not coincident for each phase. This asymmetry can also been observed on the spreading of the EMF measured for each center shift.

Furthermore, the simulated value of coefficient for the induced EMF is K_ϕ=10.6 [Vs/rad m], with an error of about 9% w.r.t. the measurements.

A second set of simulations has been performed with the windings short-circuited. In this case, the rotor is fixed in some out-centered positions dx=[0; 0.25; 0.50; 0.75; 1.0; 1.25] mm and rotates at different constant spin speeds. Figure 9 shows the time varying currents in the short-circuited windings for a center shift *dx=1 mm*, @ 7200 rpm. Figure 9 confirms the great similarity of the simulation results on each phase announced on the analysis of Fig. 7. Since the rotor spin speed has been kept constant, the transient behavior of the currents takes into account only the electrical time constant.

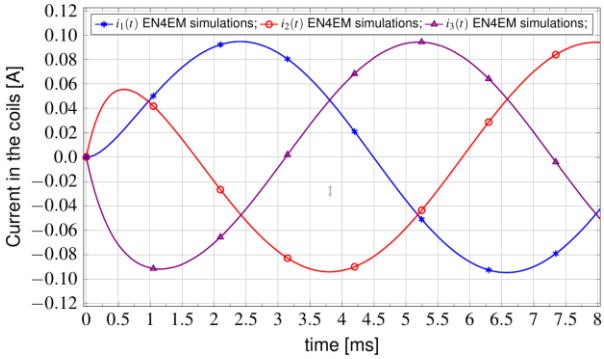

Fig. 9. Currents in the (short-circuited) coils as a function of time (dx=1mm, @7200 rpm).

In particular the reported waveforms are obtained by simultaneously shorting the three windings by closing three switches when the polar axis of the flux density distribution of the PMs on the rotor is aligned with the axis of the coils 1 and 1'. The left part of Fig. 2 shows the position of the rotor with respect to the windings at the moment of closing the switches.

We have not taken experimental measurements of the currents, but the accuracy of the computations can be indirectly assumed by the values of the forces produced by the interaction of these currents with the flux density by the PM as shown by Figs. 10 and 11.

These figures respectively show the centering $F_x(dx)$, $F_y(dy)$ (i.e., the forces acting along the direction of the displacement of the rotor) and perpendicular forces $F_x(dy)$, $F_y(dx)$ as a function of center shift *dx* or *dy*. In the same figures the experimental measurements have also been reported. The comparison shows a maximum error of about 5% for the centering force, and an error of about 10% for the perpendicular one, confirming a good agreement between the simulations results and the measurements.

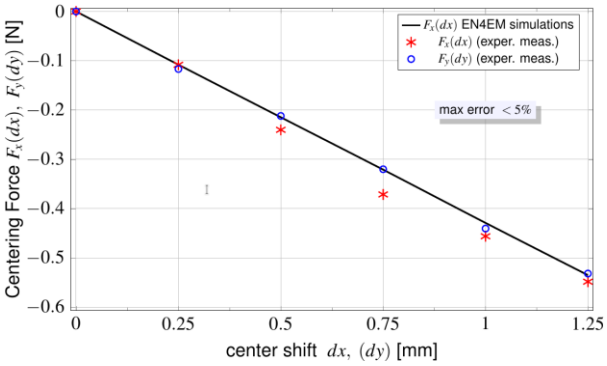

Fig. 10. Centering forces *Fx(dx)* and *Fy(dy)* as a function of center shift *dx* (@7200 rpm).

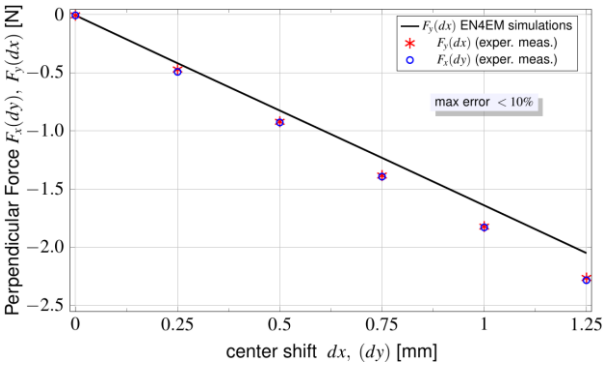

Fig. 11. Perpendicular forces *Fx(dy)*, *Fy(dx)* as a function of center shift dx (@7200 rpm).

Only one centering and one perpendicular computed forces are reported in the figures, since the others are very close to the reported ones (the differences are less than 1%). During the simulations we noticed that the perpendicular force is very sensitive to the distance between the rotor and the coils. This is due to the profile of the magnetic flux density B produced by the permanent magnet.

Figure 12 shows the profiles of the centering *Fx(dx)* and perpendicular force *Fy(dx)* for different center shifts *dx* as a function of spin speed in the range *[0 - 7200] rpm*.

About the accuracy of the computed data reported in Fig. 12, let us consider Figs. 10 and 11, which report the forces in correspondence of several displacements at the speed of *7200 rpm*. Also Figs. 13 and 14 show the comparison at the displacement of *1.25 mm* for several spin speeds. The agreement between experimental and computed data in the range of displacement and speed as in Fig. 12 is comparable with the ones shown on Figs. 10, 11, 13 and 14, and is fully satisfactory.

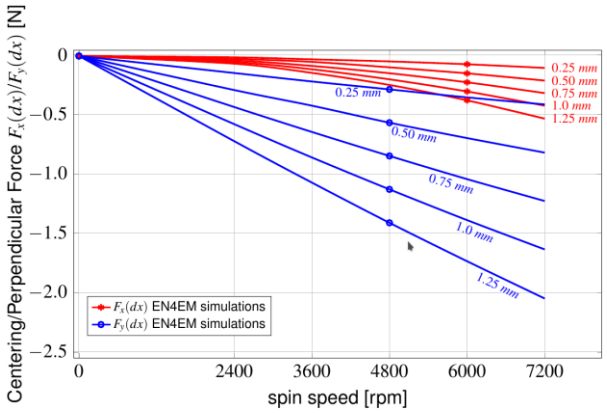

Fig. 12. Centering/perpendicular force *Fx(dx)*/*Fy(dx)* as a function of speed at different center shift *dx*.

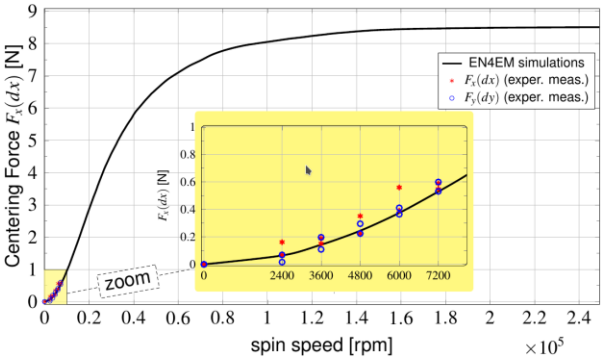

Fig. 13. Centering forces *Fx(dx)* as a function of the speed (in rpm) and with the center shift *dx = 1.25 mm*.

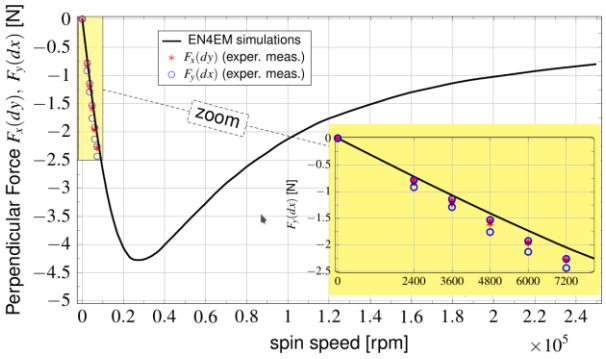

Fig. 14. Perpendicular forces *Fy(dx)* as a function of the speed (in rpm) and with the center shift *dx = 1.25 mm*.

The same figures also report the comparison with the experimental measurements in the range *[0 - 7200] rpm*, showing a good agreement. It can also be observed on these figures that at the spin speed of 7200 rpm, the parasitic force, perpendicular to the center shift is more important than the restoring force. This is due to the fact that, at that spin speed, the rotor is not spinning fast enough in comparison to the electrical pole. The restoring force becomes more important and the parasitic perpendicular force becomes smaller when the spin speed becomes higher than the electrical pole of the system [7]. For this prototype to be able to work in dynamic conditions, the spin speed should be higher, and additional external damping should also be added [8].

VI. CONCLUSIONS

A numerical analysis of a Heteropolar Electrodynamic Bearing has been presented. The simulations have been performed by the use of a numerical code based on a 3D integral formulation, previously developed at the University of Pisa for research purposes, and

capable to simulate coupled electro/mechanical problems with up to six degree of freedoms. The code shares a number of features of integral formulations, in particular the capability of producing acceptable results with very poor discretizations which require short computation times. For the magnetic bearing under test we used a model with about 500 elementary volumes which was able to produce results in very good agreement with the experimental measurements. The ongoing work is aimed to investigate the behavior of the HEDB taking into account further degrees of freedom during dynamic operation.

ACKNOWLEDGMENT

The authors would like to thank the NVIDIA's Academic Research Team for the donation of two NVIDIA Tesla K20c GPUs that have been extensively exploited for the simulations.

REFERENCES

[1] G. Schweitzer and E. H. Maslen, *Magnetic Bearings: Theory, Design and Application to Rotating Machinery*. New York, NY, USA: *Springer*, 2009.

[2] A. Looser and J. W. Kolar, "An active magnetic damper concept for stabilization of gas bearings in high-speed permanent-magnet machines," *IEEE Trans. Ind. Electron.*, vol. 61, no. 6, pp. 3089-3098, June 2014.

[3] R. F. Post and D. D. Ryutov, "Ambient-temperature passive magnetic bearings: Theory and design equations," *in Proc. 6th Int. Symp. Magn. Bearings*, pp. 110-122, Aug. 1998.

[4] S. Earnshaw, "On the nature of the molecular forces which regulate the constitution of the luminiferous ether," *Trans. Cambridge Philosoph. Soc.*, vol. 7, pp. 97-112, 1842.

[5] J. G. Detoni, "Progress on electrodynamic passive magnetic bearings for rotor levitation," *Proc. Inst. Mech. Eng. C, J. Mech. Eng. Sci.*, vol. 228, no. 10, pp. 1829-1844, 2014.

[6] C. Dumont, V. Kluyskens, and B. Dehez, "Null-flux radial electrodynamic bearing," *IEEE Trans. Magn.*, vol. 50, no. 10, Oct. 2014.

[7] N. Amati, X. De Lépine, and A. Tonoli, "Modeling of electrodynamic bearings," *J. Vibrat. Acoust.*, vol. 130, no. 6, p. 061007, Oct. 2008.

[8] V. Kluyskens and B. Dehez, "Dynamical electromechanical model for magnetic bearings subject to eddy currents," *IEEE Trans. Magn*., vol. 49, no. 4, pp. 1444-1452, Apr. 2013.

[9] A. V. Filatov and E. H. Maslen, "Passive magnetic bearing for fly-wheel energy storage systems," *IEEE Trans. Magn.*, vol. 37, no. 6, pp. 3913-3924, Nov. 2001.

[10] J. G. Detoni, F. Impinna, A. Tonoli, and N. Amati, "Unified modelling of passive homopolar and heteropolar electrodynamic bearings," *J. Sound Vibrat.*, vol. 331, no. 19, pp. 4219-4232, Sep. 2012.

[11] A. Rahideh and T. Korakianitis, "Analytical open-circuit magnetic field distribution of slotless brushless permanent-magnet machines with rotor eccentricity," *IEEE Trans. Magn*., vol. 47, no. 12, pp. 4791-4808, Dec. 2011.

[12] A. Tonoli, N. Amati, F. Impinna, J. G. Detoni, H. Bleuler, and J. Sandtner, "Dynamic modeling and experimental validation of axial electrodynamic bearings," in *Proc. of the 12th Int. Symposium on Magnetic Bearings*, p. 68-73, 2011.

[13] B. Davat, Z. Ren, and M. Lajoie-Mazenc, "The movement in field modeling," *IEEE Trans. on Mag.*, vol. 21, no. 6, pp. 2296-2298, Nov. 1985.

[14] A. Bossavit, *Computational Electromagnetism: Variational Formulations, Complementarity, Edge Elements*. Academic Press, 1998.

[15] D. Rodger, H. C. Lai, and P. J. Leonard, "Coupled elements for problems involving movement," *IEEE Trans. on Mag.*, vol. 26, no. 2, pp. 548-550, Mar. 1990.

[16] R. Albanese and G. Rubinacci, "Integral formulation for 3D eddy-current computation using edge elements," *IEEE Proceedings A (Physical Science, Measurement and Instrumentation, Management and Education, Reviews)*, vol. 135, no. 7, pp. 457-462, 1988.

[17] E Tripodi, A Musolino, R Rizzo, and M Raugi, "A new predictor-corrector approach for the numerical integration of coupled electromechanical equations," *Int. J. for Num. Meth. in Eng*., vol. 105, no. 4 pp. 261-285, 2016.

[18] A. Musolino, R. Rizzo, M. Toni, and E. Tripodi, "Modeling of electromechanical devices by GPU-accelerated integral formulation," *Int. Jour. of Num. Mod. in Electron. Network, Dev. and Field*, vol. 26, pp. 376-396, 2013.

[19] V. Di Dio and L. Sani, "Coupled electromechanical analysis of a permanent-magnet bearing," *ACES Journal*, vol. 32, no. 8, pp. 736-741, Aug. 2017.

[20] M. G. Iachininoto, et al., "Effects of exposure to gradient magnetic fields emitted by nuclear magnetic resonance devices on clonogenic potential and proliferation of human hematopoietic stem cells," *Bioelectromagnetics*, vol. 37, no. 1 pp. 201-211, 2016.

[21] C. Dumont, V. Kluyskens, and B. Dehez, "Design and experimental testing of a heteropolar electrodynamic bearing," *2nd IEEE Conference on Advances in Magnetics*, LaThuile, Italy, Feb. 2018.